Journal of ELECTRONIC MATERIALS, Vol. 41, No. 6, 2012
DOI: 10.1007/s11664-012-1931-y

Facile Preparation and Characterization of Poly (3-hexylthiophene)/Multiwalled Carbon Nanotube Thermoelectric Composite Films

Y. DU,[1,2] S.Z. SHEN,[2] W.D. YANG,[2] S. CHEN,[1] Z. QIN,[1] K.F. CAI,[1,3] and P.S. CASEY[2]

1.—Functional Materials Research Laboratory, Tongji University, 1239 Siping Road, Shanghai 200092, China. 2.—Materials Science and Engineering Division, CSIRO, Private Bag 33, Clayton South, 3169 Victoria, Australia. 3.—e-mail: kfcai@tongji.edu.cn

This paper reports a novel, cost-effective, scalable, and simple method for preparing poly(3-hexylthiophene)/multiwalled carbon nanotube (P3HT/MWCNT) nanocomposite films. The P3HT/MWCNT films were prepared by oxidative polymerization of 3-hexylthiophene in chloroform solution containing dispersed MWCNT. The phase composition and microstructure of the composite films were analyzed by x-ray diffraction (XRD), Fourier-transform infrared spectroscopy, Raman spectroscopy, thermogravimetric analysis, and field-emission scanning electron microscopy. The composite films were smooth, dense, and uniform. The thermoelectric properties of the composite films were measured at room temperature. The electrical conductivity and Seebeck coefficient of the films with MWCNT content of 5 wt.% were $\sim 1.3 \times 10^{-3}$ S/cm and 131.0 μV/K, respectively.

Key words: Poly(3-hexylthiophene), multiwalled carbon nanotubes, thermoelectric properties, nanocomposite, film

INTRODUCTION

Solid-state cooling and power generation based on thermoelectric (TE) effects have potential applications in waste heat recovery, air conditioning, and refrigeration. The TE performance of a material is evaluated by the material's dimensionless figure of merit ZT ($=\alpha^2\sigma T/\kappa$, where α is the Seebeck coefficient, σ is the electrical conductivity, κ is the thermal conductivity, and T is the absolute temperature). To obtain high ZT, it is necessary to optimize these parameters simultaneously. However, as α, σ, and κ are interdependent, changing one alters the others, making optimization extremely difficult.[1]

Bismuth telluride (Bi_2Te_3)-based alloys are the best commercially available inorganic TE materials ($ZT \approx 1$ near room temperature). The predominant techniques used to prepare Bi_2Te_3-based nanopowders are rapid solidification,[2] atomization,[3] ball milling,[4] surfactant directed synthesis,[5] and thermolysis reduction methods.[6] Expensive raw materials and facilities for fabrication, heavy-metal pollution, and poor processability limit their wide application.[7–10] Consequently, developing high performance with relatively economical TE materials is of key importance if the benefits of their properties are to be realized.[7,11]

Conducting polymers are important materials which can be applied in the field of sensors, energy storage, corrosion inhibition, enzyme activity, electronic, and optoelectronic devices. Recently, increasing attention has focused on the TE properties of conducting polymers that have relatively high chemical stability in ambient conditions, low density, low thermal conductivity, low cost, and ease of synthesis and processing into versatile forms. Such polymers include β-naphthalene sulfonic acid-doped polyaniline (PANI) nanotubes,[12] poly(3-hexylthiophene) (P3HT) film,[13] poly(3,4-ethylenedioxythiophene) (PEDOT) nanowires,[14] PEDOT-tosylate films,[15] as well as PEDOT nanotubes.[16] Much progress has

(Received July 16, 2011; accepted January 12, 2012; published online February 23, 2012)

been made with some of these polymers and polymer-based nanocomposites.[7,11,16–20]

Carbon nanotubes (CNTs) are renowned for their extraordinary electrical, mechanical, and thermal properties. Furthermore, CNTs are nanosize and have holey structure features which are beneficial to achieving high *ZT*. Consequently, they are promising candidates for TE materials in view of the quantum confinement effect of the charge carriers and the size effect of the heat carriers.[21] Yu et al.[11] reported that, when CNTs were incorporated into a polymer matrix, as the CNT concentration increased, the electrical conductivity of the composite increased dramatically while the thermal conductivity and Seebeck coefficient remained relatively unchanged. This behavior results from thermally disconnected but electrically connected junctions, making it feasible to tune properties in favor of higher *ZT*. Subsequently, several studies examining the TE properties of polymer/CNTs composites have been reported, such as PANI-coated CNT sheet,[18] PANI/single-walled carbon nanotube (SWCNT) composite,[7] and poly(3,4-ethylenedioxythiophene): poly(styrenesulfonate) (PEDOT:PSS)/CNT composite.[20] The Seebeck coefficients of these composites were relatively low (~11 μV/K to 50 μV/K). However, more recently, Sun et al.[13] reported that tetrafluorotetracyanoquinodimethane (F_4TCNQ)-doped P3HT film had a much larger Seebeck coefficient (~400 μV/K to 580 μV/K).

Preparation of P3HT/CNT nanocomposites may be an effective route to produce relatively low-density, high-performance TE materials, by taking advantage of the properties of CNT (high electrical conductivity) and P3HT (low thermal conductivity) to potentially have a synergistic effect. To the best of our knowledge, no research on the TE properties of P3HT/MWCNT nanocomposite films has been reported. In this work, P3HT/MWCNT TE composite films were prepared and the TE properties of the prepared films were investigated.

EXPERIMENTAL PROCEDURES

Raw Materials

3-Hexylthiophene (3HT) monomer (97%), chloroform, anhydrous iron (III) chloride (oxidant), and other organic solvents were purchased from Sigma–Aldrich Chem. Co (reagent grade). MWCNT (main range of diameter: 10 nm to 20 nm, length: 5 μm to 15 μm, purity: ≥95%) were purchased from Shenzhen Nanotech Port Co., Ltd. All of these were used without further purification.

Preparation of P3HT-MWCNT Films

A typical procedure for preparing P3HT/MWCNT films was as follows: 100 mL $CHCl_3$ solution containing MWCNT (5 wt.% with respect to the 3HT monomer weight) was placed in a 500-mL beaker and then sonicated for 1 h at room temperature (solution A). Secondly, 0.168 g (1 mmol) 3HT monomer dissolved in 50 mL $CHCl_3$ solution was added to solution A and further sonicated for 30 min (solution B). Then, 0.649 g (4 mmol) $FeCl_3$ was dissolved in 50 mL $CHCl_3$ solution and added through a separating funnel to solution B, then continuously stirred at constant rate for 24 h at room temperature. The resultant P3HT/MWCNT composite was precipitated in methanol and then centrifuged for 10 min at 3000 rpm. When centrifuging was finished, the composite formed a layer on the bottom of the flask. After separating the methanol, the composite was carefully washed with distilled water without stirring, followed by centrifuging. The upper water was then removed. This washing step was repeatedly many times until the upper solution became colorless. Finally, the product was dried (in the centrifuge container) under vacuum at 60°C. A P3HT/MWCNT composite film was obtained at the bottom of the container. A pure P3HT film, containing no nanotubes, was synthesized using the same procedure as described above for comparison. The process for preparation of P3HT/MWCNT composite films is schematically depicted in Fig. 1.

Characterization

The molecular weight of the prepared P3HT film was measured using gel permeation chromatography (GPC) in tetrahydrofuran (THF) at 30°C. The prepared P3HT/MWCNT composite film was examined by x-ray diffraction (XRD, Bruker D8 Advance) with Cu K_α radiation (λ = 1.5406 Å), Fourier-transform infrared spectroscopy (FTIR, Nicolet 6700, spectral range: 650 cm^{-1} to 10,000 cm^{-1}), and Raman spectroscopy (Nicolet Almega XR model) using a laser diode at excitation wavelength of 514 nm and 10% laser power level. The thermal stability of the film was examined by thermal gravimetric analysis (TGA) using a Pyris 1 TGA under nitrogen atmosphere at heating rate 10°C/min. The morphology of the film was observed by field-emission scanning electron microscopy (FE-SEM) using a Quanta 200 FEG.

The electrical conductivity and Seebeck coefficient of the film were measured at room temperature. A standard four-probe method was used for the electrical conductivity measurement, while the Seebeck coefficient was determined from the slope of the linear relationship between the thermoelectromotive force and temperature difference (~10 K) between two points on the film.

RESULTS AND DISCUSSION

The molecular weights determined by GPC were 167,536 (M_w) and 53,657 (M_n) for the P3HT film, with 3.12 as a measure of polydispersity. The M_w and M_n of the prepared P3HT film were greater than those reported in Ref. 22 (39,717 and 12,778, respectively, polydispersity = 3.11).

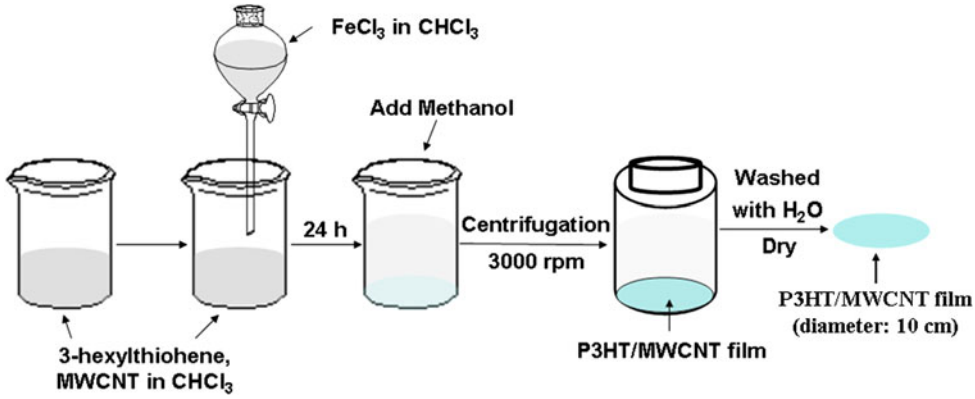

Fig. 1. Illustration of the process for preparation of P3HT/MWCNT composite film.

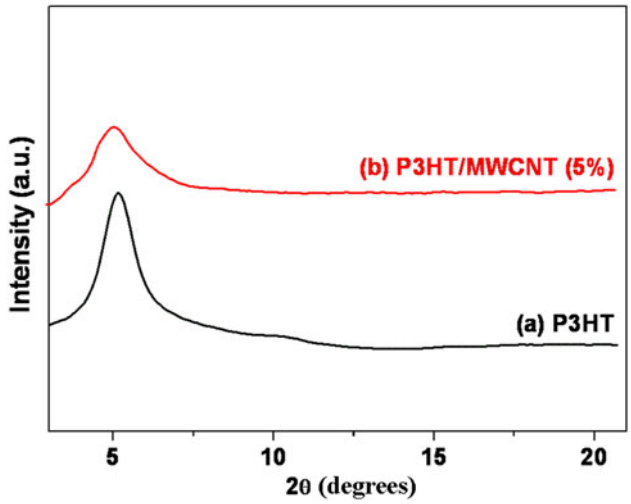

Fig. 2. XRD patterns of (a) P3HT and (b) P3HT/MWCNT composite films.

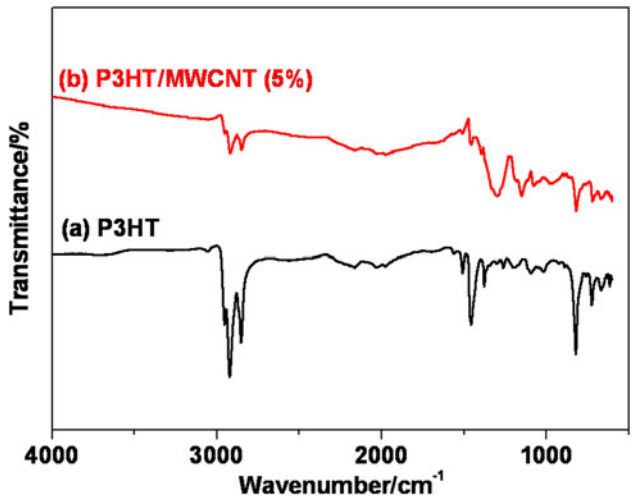

Fig. 3. FTIR spectra of (a) P3HT and (b) P3HT/MWCNT composite films.

XRD patterns of the P3HT and P3HT/MWCNT composite films are presented in Fig. 2. For P3HT, the peak at $2\theta = 5.15°$ corresponds to $d = 17.13$ Å, which is the in-plane interchain distance between thiophene rings, and the weak peak at $2\theta = 10.24°$ corresponds to $d = 8.596$ Å, representing second-order reflections from the interlayer spacing.[22] When compared with the XRD pattern of the P3HT film, the P3HT/MWCNT composite film showed a similar XRD pattern but with a weaker and wider XRD peak, indicating that the polymorphic nature of the P3HT remained unchanged[23] and that the size of the P3HT in the P3HT/MWCNT composite film was smaller.

Figure 3 shows the FTIR spectra of P3HT and P3HT/MWCNT composite films. For P3HT, all the peaks agree with the results reported in Ref. 22. The absorption peaks at 3053 cm^{-1} and 2955 cm^{-1} are attributed to the C_β–H aromatic stretching mode and the $–CH_3$ asymmetry stretch vibration, respectively; those at 2922 cm^{-1} and 2853 cm^{-1} to the $–CH_2–$ stretch vibration, those at 1378 cm^{-1} to the $–CH_3$ bending vibration,[24] and those at 1150 cm^{-1} and 720 cm^{-1} to the characteristic out-of-plane and in-plane rocking vibration of $–(CH_2)_n–$ group ($n \geq 4$).[24] The absorption peak at approximately 1455 cm^{-1} belongs to the symmetric C=C stretch, while the antisymmetric stretch of this vibration (1508 cm^{-1}), which is very weak in the P3HT, is not shifted in the P3HT/MWCNT composite films. These results suggest that there was no strong interaction between the P3HT and the MWCNT but only simple π–π stacking.[22]

Raman spectroscopy is sensitive to both electronic and vibrational structures of carbon nanotubes and has been used to probe the structure of polymer nanocomposites.[24] In the present case, Raman spectroscopy of MWCNT powder and the as-prepared P3HT and P3HT/MWCNT films was performed, and the results are presented in Fig. 4. The peaks at 1380 cm^{-1} and 1448 cm^{-1} correspond to the thiophene ring mode of regioregular P3HT.[25]

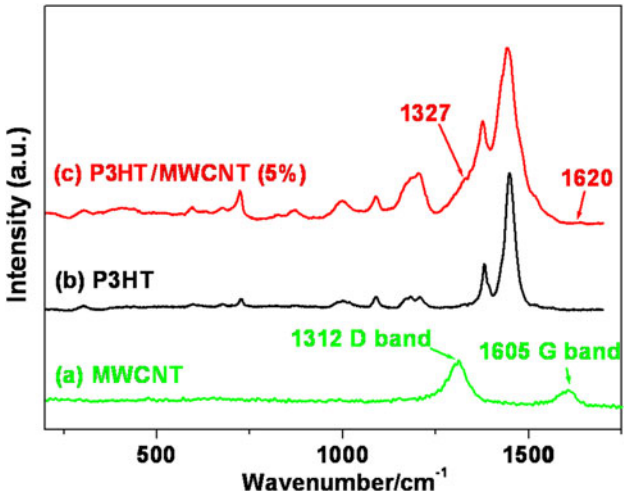

Fig. 4. Raman spectra of (a) MWCNT powder, and (b) P3HT and (c) P3HT/MWCNT composite films.

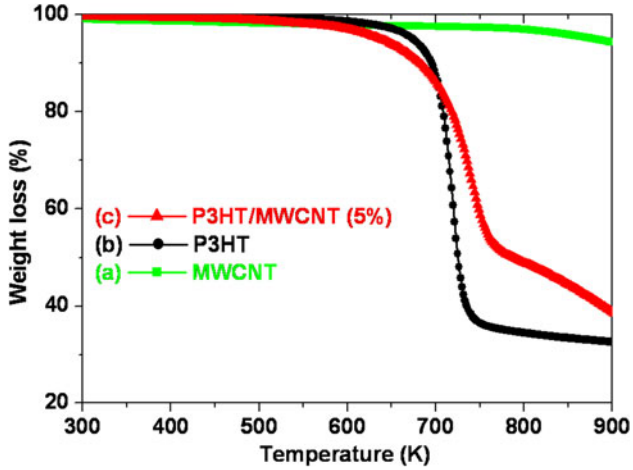

Fig. 5. TGA curves of (a) MWCNT powder, and (b) P3HT and (c) P3HT/MWCNT composite films.

In the MWCNT trace, the important peaks at 1312 cm^{-1} and 1605 cm^{-1} correspond to the sp^3 mode (D band) and the tangential mode (G band) of the nanotubes, respectively.[26] A redshift (~15 cm^{-1}) of the MWCNT peaks was observed in the P3HT/MWCNT composite films, which agrees with results reported in Ref. 25 Possible reasons for this may be (i) the MWCNTs donate electronic charge to the P3HT matrix,[27] and (ii) because the MWCNT content was low (5 wt.%), most of their surface is likely covered by P3HT matrix. Consequently, the freedom of the C–C vibration on the graphene plane will be restricted due to CH–π interactions (CH–π interactions observed between nanotube and P3HT are stronger than π–π interactions observed between nanotube bundles).[28] A similar redshift of the G band (~17 cm^{-1}) has also been reported for SWCNT/polypropylene[29] and SWCNT/reinforced epoxy resins.[30]

The TGA results of P3HT and P3HT/MWCNT composites compared with pure MWCNT powder are presented in Fig. 5. MWCNT powder was more stable than the composite samples in the temperature range of 300 K to ~900 K, with the higher residual weight of MWCNTs due to the presence of undegraded MWCNT. Degradation typically starts at ≥873 K.[31] The P3HT and P3HT/MWCNT composite films started degrading at 664 K and 648 K, respectively. When the content of MWCNT is 5%, P3HT/MWCNT composite films have lower thermal stability than that of pure P3HT, which agrees with the result reported in Ref. 23.

Figure 6 shows FESEM images of the prepared P3HT/MWCNT composite film. Top-view FESEM observation indicates that the P3HT/MWCNT film is dense and has a smooth surface with uniform morphology, similar to the P3HT film reported in Ref. 22, but it is difficult to see the MWCNT in the P3HT matrix (possibly because the MWCNT content is very low). FESEM images of the fracture surface of the film, however, clearly show the wire-like nanostructure of the MWCNT in the P3HT matrix (Fig. 6d).

The electrical conductivity of the P3HT/MWCNT composite film is ~1.3 × 10^{-3} S/cm, which is greater than that of the pure P3HT film (2.5 × 10^{-6} S/cm) prepared under the same procedure and higher than that of the F_4TCNQ-doped P3HT film (~1.8 × 10^{-5} S/cm to 3.8 × 10^{-5} S/cm).[13] This value is also higher than that of P3HT/double-walled carbon nanotube (DWCNT) composites (5.3 × 10^{-4} S/cm, with 5 wt.% DWCNT)[22] and poly(3-octylthiophene)/SWCNT composites[24] (5.4 × 10^{-6} S/cm, with 5 wt.% SWCNT). This may be because the as-prepared P3HT/MWCNT composite films have a smooth, dense, uniform morphology. However, the electrical conductivity of the P3HT/MWCNT composite film is still lower than that of PANI-coated CNT sheet (~30 S/cm to 90 S/cm),[18] PANI/SWCNT composite (~10 S/cm to 125 S/cm),[7] PEDOT:PSS/CNT composite (~0 S/cm to 124 S/cm),[20] and poly(vinyl acetate)/CNT composite (~0 S/cm to 48 S/cm).[11] The main reason might be that the electrical conductivity of PANI and PEDOT:PSS is much higher than that of pure P3HT.

The Seebeck coefficient of the prepared P3HT/MWCNT composite film is ~131.0 μV/K (see plot of thermoelectromotive force versus temperature difference from two points on the film in Fig. 7; the Seebeck coefficient of the pure P3HT film could not be measured, probably due to its low electrical conductivity), indicating that the film is a *p*-type conductor. The Seebeck value is much higher than that of PANI-coated CNT sheet (~12 μV/K to 28 μV/K),[18] PANI/SWCNT composite (~11 μV/K to 40 μV/K),[7] PEDOT:PSS/CNT composite (~17 μV/K to 40 μV/K),[20] and poly(vinyl acetate)/CNT composite (~40 μV/K to 50 μV/K),[11] but smaller than that of F_4TCNQ-doped P3HT film (~400 μV/K to 580 μV/K).[13] This means that the preparation route reported in this paper for polymer/CNT films can

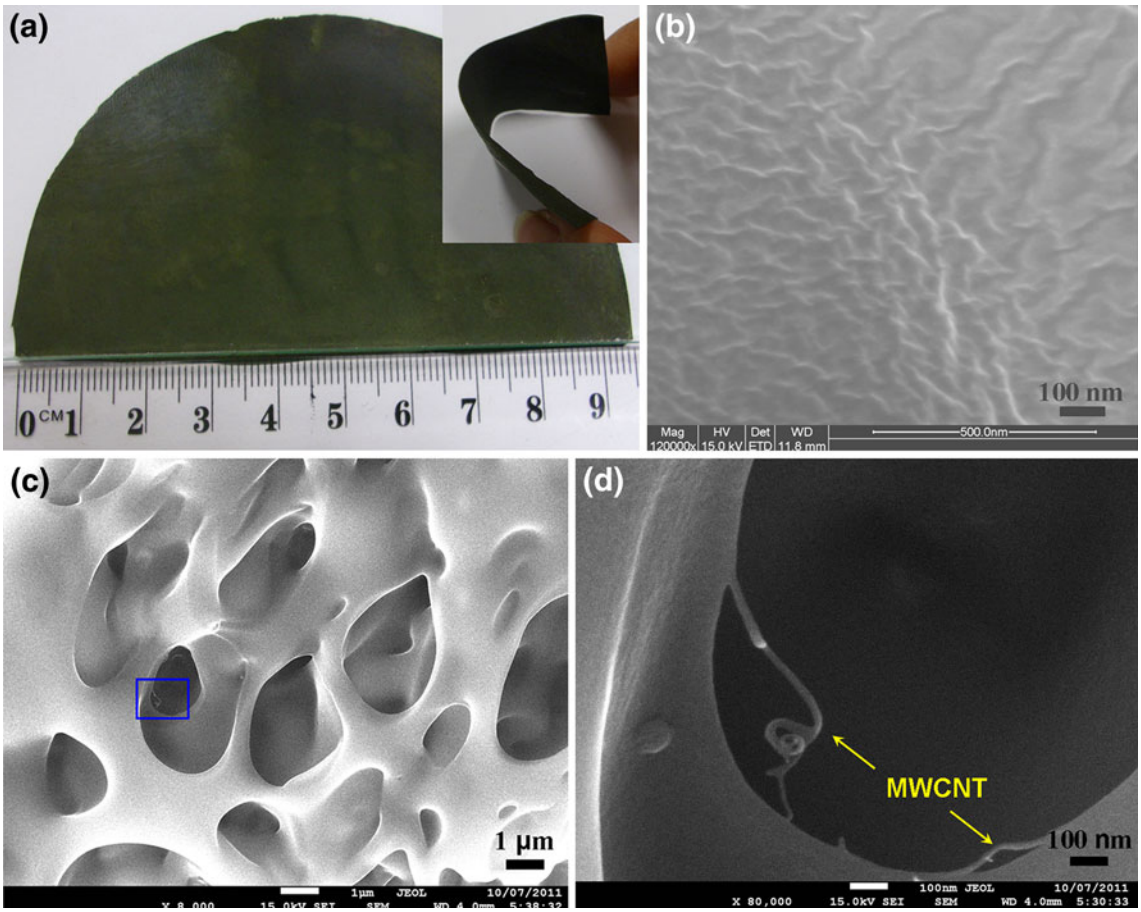

Fig. 6. Photograph of the prepared P3HT/MWCNT composite film (a); the inset in (a) shows a bent strip of the prepared film. (b) Top-view FESEM image of the P3HT/MWCNT composite film. (c) FESEM image of the fracture surface of the film, and (d) high-magnification FESEM image of the area marked by a square in (c).

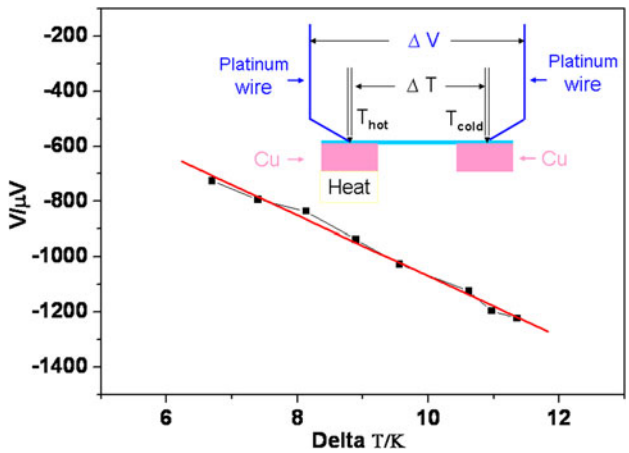

Fig. 7. Thermoelectromotive force versus temperature difference from two points on the film. Inset is a schematic diagram of the Seebeck coefficient measurement.

significantly increase the electrical conductivity while maintaining the Seebeck coefficient at a high value. Furthermore, given the low thermal conductivity of these composite films, a high *ZT* value can be expected. The TE properties of the film may be further improved by adjusting the MWCNT content and by doping with dopants such as I_2 or F_4TCNQ.

CONCLUSIONS

Smooth, dense, and uniform P3HT/MWCNT films were prepared. For MWCNT content of 5 wt.%, the electrical conductivity and Seebeck coefficient were $\sim 1.3 \times 10^{-3}$ S/cm and 131.0 μV/K, respectively. The preparation route for the P3HT/MWCNT film is novel, cost-effective, scalable, and simple. This route has potential for use in other polymer systems.

ACKNOWLEDGEMENTS

This work was supported by National Natural Science Foundation of China (50872095). Y.D. would like to thank China Scholarship Council for the financial support for his study at CSIRO, Australia. We acknowledge use of the facilities and the assistance of Dr. Xiya Fang at the Monash Centre for Electron Microscopy. We would also like to thank Dr. Deborah Lau and Dr. Adrian Trinchi at Materials Science and Engineering Division, CSIRO, for Raman spectra analysis.

REFERENCES

1. A. Majumdar, *Science* 303, 777 (2004).
2. J.Y. Kim, J.H. Jung, D.E. Lee, and J. Joo, *Synth. Met.* 126, 311 (2002).
3. K. Yanagimoto, K. Majima, S. Sunada, and T. Sawada, *J. Alloys Compd.* 377, 174 (2004).
4. J.Y. Yang, T. Aizawa, A. Yamamoto, and T. Ohta, *J. Alloys Compd.* 312, 326 (2000).
5. A. Purkayastha, Q.Y. Yan, M.S. Raghuveer, D.D. Gandhi, H.F. Li, Z.W. Liu, R.V. Ramanujan, T. Borca-Tasciuc, and G. Ramanath, *Adv. Mater.* 20, 2679 (2008).
6. L.X. Bu, W. Wang, and H. Wang, *Appl. Surf. Sci.* 253, 3360 (2007).
7. Q. Yao, L.D. Chen, W.Q. Zhang, S.C. Liufu, and X.H. Chen, *ACS Nano* 4, 2445 (2010).
8. N. Toshima, *Macromol. Symp.* 186, 81 (2002).
9. F.J. DiSalvo, *Science* 285, 703 (1999).
10. J.J. Li, X.F. Tang, H. Li, Y.G. Yan, and Q.J. Zhang, *Synth. Met.* 160, 1153 (2010).
11. C. Yu, Y.S. Kim, D. Kim, and J.C. Grunlan, *Nano Lett.* 8, 4428 (2008).
12. Y.M. Sun, Z.M. Wei, W. Xu, and D.B. Zhu, *Synth. Met.* 160, 2371 (2010).
13. J. Sun, M.L. Yeh, B.J. Jung, B. Zhang, J. Feser, A. Majumdar, and H.E. Katz, *Macromolecules* 43, 2897 (2010).
14. D.K. Taggart, Y.A. Yang, S.C. Kung, T.M. McIntire, and R.M. Penner, *Nano Lett.* 11, 125 (2011).
15. O. Bubnova, Z.U. Khan, A. Malti, S. Braun, M. Fahlman, M. Berggren, and X. Crispin, *Nat. Mater.* 10, 429 (2011).
16. Y.Y. Wang, K.F. Cai, and X. Yao, *ACS Appl. Mater. Interfaces* 3, 1163 (2011).
17. Y.Y. Wang, K.F. Cai, J.L. Yin, B.J. An, Y. Du, and X. Yao, *J. Nanopart. Res.* 13, 533 (2011).
18. C.Z. Meng, C.H. Liu, and S.S. Fan, *Adv. Mater.* 22, 535 (2010).
19. Y. Du, K.F. Cai, Z. Qin, S.Z. Shen, and P.S. Casey, *Conference on Mechanical, Industrial, and Manufacturing Engineering (MIME 2011); Australia, Melbourne* (2011), p. 462.
20. D. Kim, Y. Kim, K. Choi, J.C. Grunlan, and C. Yu, *ACS Nano* 4, 513 (2010).
21. J.P. Small, L. Shi, and P. Kim, *Solid State Commun.* 127, 181 (2003).
22. R. Koizhaiganova, H.J. Kim, T. Vasudevan, S. Kudaibergenov, and M.S. Lee, *J. Appl. Polym. Sci.* 115, 2448 (2010).
23. B.K. Kuila, S. Malik, S.K. Batabyal, and A.K. Nandi, *Macromolecules* 40, 278 (2007).
24. H.J. Kim, R.B. Koizhaiganova, M. Karim, G.H. Lee, T. Vasudevan, and M.S. Leel, *J. Appl. Polym. Sci.* 118, 1386 (2010).
25. A.W. Musumeci, G.G. Silva, J.W. Liu, W.N. Martens, and E.R. Waclawik, *Polymer* 48, 1667 (2007).
26. Y.L. Liu and W.H. Chen, *Macromolecules* 40, 8881 (2007).
27. K.E. Wise, C. Park, E.J. Siochi, and J.S. Harrison, *Chem. Phys. Lett.* 391, 207 (2004).
28. D. Baskaran, J.W. Mays, and M.S. Bratcher, *Chem. Mat.* 17, 3389 (2005).
29. L. Valentini, J. Biagiotti, J.M. Kenny, and S. Santucci, *Compos. Sci. Technol.* 63, 1149 (2003).
30. V.G. Hadjiev, M.N. Iliev, S. Arepalli, P. Nikolaev, and B.S. Files, *Appl. Phys. Lett.* 78, 3193 (2001).
31. Z.Q. Peng, A.H. Holm, L.T. Nielsen, S.U. Pedersen, and K. Daasbjerg, *Chem. Mat.* 20, 6068 (2008).